

# Coarse-graining polymers as soft colloids

A.A. Louis,<sup>a,\*</sup> P.G. Bolhuis,<sup>b</sup> R. Finken,<sup>a</sup> V. Krakoviack,<sup>a</sup>  
E.J. Meijer,<sup>b</sup> J.P. Hansen<sup>a</sup>

<sup>a</sup>*Department of Chemistry, Lensfield Rd, Cambridge CB2 1EW, UK*

<sup>b</sup>*Department of Chemical Engineering, University of Amsterdam, Nieuwe  
Achtergracht 166, NL-1018 WV Amsterdam, Netherlands*

---

## Abstract

We show how to coarse grain polymers in a good solvent as single particles, interacting with density-independent or density-dependent interactions. These interactions can be between the centres of mass, the mid-points or end-points of the polymers. We also show how to extend these methods to polymers in poor solvents and mixtures of polymers. Treating polymers as soft colloids can greatly speed up the simulation of complex many-polymer systems, including polymer-colloid mixtures.

*Key words:* Polymer solutions; Colloids; Effective interactions

*PACS:* 61.25.H, 61.20.Gy, 82.70Dd

---

## 1 Introduction

Binary mixtures of colloidal particles and non-adsorbing polymers have received renewed and growing attention recently, in part because they exhibit complex and interesting structure, phase behaviour, interfacial properties, and rheology [1–6], and in part because they are excellent model systems for the study of large length and time-scale separations in complex fluids. Problems with bridging length-scales are immediately apparent in even the simplest models of colloid-polymer mixtures: while the mesoscopic colloidal particles can be modeled as hard convex bodies, the polymers are generally treated at the microscopic (Kuhn) segment level. Thus, even though the average size of the polymer coils may be of the same order of magnitude as that of the colloids, the number of degrees of freedom needed to model the former may be several

---

\* Corresponding author. Tel.: +44-1223-336535; fax: +44-1223-336362  
*Email address:* aal20@cus.cam.ac.uk (A.A. Louis).

orders of magnitude larger than what is needed for the latter. This naturally provokes the question: Can the polymers also be modeled as single particles? In fact, this is exactly what was done by Asakura and Oosawa (AO) who, in their classic work on colloid polymer mixtures[7], modeled the polymers as ideal particles with respect to each other, and as hard-spheres with respect to the colloids. This model is strictly speaking only valid for non-interacting polymers, or for interacting polymers in the dilute limit, while many interesting phenomena, such as polymer induced phase separation, take place at finite concentration of interacting polymers. Our ultimate goal, therefore, is to go well beyond the AO model and describe non-ideal polymers in a good solvent up to semi-dilute concentrations. We recently extended the AO concept to take into account polymer-polymer interactions, first by rather naively assuming a Gaussian repulsion between polymers[8] to account for the penetrable nature of polymer coils, and then by carrying out a more sophisticated programme which resulted in density-dependent[9–11] and density-independent[12] interactions between polymer coils.

The next sections will examine these effective potentials in more detail.

## 2 Coarse-graining homogeneous polymer solutions

Polymers made up  $L$  segments are characterized by their radius of gyration,  $R_g \sim L^\nu$ , where  $\nu \approx 0.59$ , i.e. polymers are fractal objects. Much of our understanding of polymer solutions comes from the scaling arguments pioneered by de Gennes[13]. These arguments suggest that the behaviour of a polymer solution differs in the dilute regime, where the polymer coil density  $\rho < \rho^* = \frac{4}{3}\pi R_g^3$ , from the semi-dilute regime, where  $\rho/\rho^* \gg 1$ . Both these regimes presume that the actual monomer concentration  $c$  remains very low. Once  $c$  becomes appreciable, one enters the so-called melt regime which will not be treated here, and for which different kinds of coarse-graining methods are necessary.

A standard scaling argument suggest that the radius of gyration  $R_g$  is the only relevant lengthscale for the dilute and semi-dilute regimes of polymers in a good solvent[13]. This immediately implies that the second-virial coefficient should scale as  $B_2 \sim R_g^3$ . If we set  $x = r/R_g$  then the second-virial coefficient is proportional to

$$B_2 \sim R_g^3 \int \{1 - \exp[-\beta V(x)]\} d\mathbf{x} \quad (1)$$

where  $\beta V(x)$  is the interaction between two separate polymers, defined w.r.t. some yet to be specified coordinate. Since this must hold for all  $R_g$ , the in-

interaction  $\beta V(r/R_g)$  should not depend on the length  $L$  for sufficiently long  $L$  (scaling limit). A more sophisticated version of this argument was put forward by Grosberg, Khalatur, and Khokhlov[14], see also the review by Likos[6] for a historical overview.

To coarse-grain each polymer as a single entity, one must still choose an interaction centre, which may be the centre of mass (CM), the mid-point, the end-points, or some average monomer. For the mid-point or end-point representation,  $\beta V(x)$  should diverge at the origin, since the actual segments of two different polymers cannot overlap. For the CM, we expect a finite value of  $\beta V(x = 0)$ , since it is possible for two polymers to deform around each other in such a way that their CM coincide without any mutually avoiding monomers overlapping.

## 2.1 Density-independent polymer-polymer interactions

In the description of atomic and molecular liquids and solids it is common to replace the full quantum mechanical treatment of the interactions by a simplified effective potential. Well known examples include the Lennard Jones pair potential and the Axilrod-Teller three-body potential[15]. Here we attempt a similar coarse-graining for polymer solutions and choose the constituents to be single polymers, with a specified interaction centre for each polymer. Then, following for example [5,6] or more specifically [11], the coarse-grained Helmholtz free energy  $F$  of a set of  $N$  polymers with their interaction centres fixed at the coordinates  $\{\mathbf{r}_i\}$ , in a volume  $V$ , can be written as the following expansion:

$$F(N, V, \{\mathbf{r}_i\}) = F^{(0)}(N, V) + \sum_{i_1 < i_2}^N w^{(2)}(\mathbf{r}_{i_1}, \mathbf{r}_{i_2},) \quad (2)$$

$$+ \sum_{i_1 < i_2 < i_3}^N w^{(3)}(\mathbf{r}_{i_1}, \mathbf{r}_{i_2}, \mathbf{r}_{i_3}) + \dots + w^{(N)}(\mathbf{r}_{i_1}, \mathbf{r}_{i_2} \dots \mathbf{r}_{i_N})$$

where the coordinates of the interaction centres of the polymers,  $\{\mathbf{r}_{i_1}, \mathbf{r}_{i_2} \dots \mathbf{r}_{i_n}\}$ , are expressed in units of  $R_g$ , the radius of gyration at zero density. Each term in this coarse-grained free energy includes an implicit statistical average over all the internal monomeric degrees of freedom for a fixed configuration  $\{\mathbf{r}_i\}$ .  $F^{(0)}(N, V)$  is the so-called volume term[6], the contribution to the free energy that is independent of the configuration  $\{\mathbf{r}_i\}$ , and includes the internal free-energy of an isolated polymer. For a homogeneous solution, translational invariance implies that there is no one-body term in the expansion. Each subsequent term  $w^{(n)}(\mathbf{r}_{i_1}, \mathbf{r}_{i_2} \dots \mathbf{r}_{i_n})$  is defined as the free energy of  $n$  polymers with their interaction positions at  $\{\mathbf{r}_{i_1}, \mathbf{r}_{i_2} \dots \mathbf{r}_{i_n}\}$ , minus the contributions of

all lower order terms. This procedure may in principle be followed to derive higher and higher order interactions, until, for a system with  $N$  polymers, the  $N$ th term determines the total coarse-grained free energy. The thermodynamic free energy of the polymer solution finally follows from a statistical average over the interaction coordinates:

$$\beta F(N, V) = -\ln \sum_{\{\mathbf{r}_i\}} \exp [-\beta \mathbf{F}(N, V, \{\mathbf{r}_i\})]. \quad (3)$$

But in practice, this approach is not often feasible because the number of  $n$ -tuple coordinates and related complexity of each higher order term increases rapidly with  $n$ , so that the series in Eq. (2) and the full average in Eq. (3) quickly become intractable. Instead, one hopes to show that the series converges fast enough that only a few low order terms are needed to obtain a desired accuracy.

The first important term in the series expansion is the pair interaction  $w^{(2)}(r)$ , which can be determined by calculating the logarithm of the probability that two polymers have their interaction centres a distance  $r$  apart. Details of our computer simulation technique are described elsewhere[10,11,16]. In brief, by simulating  $L = 500$  self-avoiding walk (SAW) polymers on a cubic lattice, we determined  $w^{(2)}(r)$  for three different interaction centres: the end-points, mid-point, and CM of each polymer, as depicted in Fig 2. The end and mid-point representations diverge at the origin as  $\lim_{r \rightarrow 0} w^{(2)}(r) \sim \ln(r/R_g)$ [6], while the CM representation has a finite value which we estimate to be  $w^{(2)}(0) = 1.80 \pm 0.05$  in the scaling limit  $L \rightarrow \infty$ [10]. By plotting  $r^2 v(r)$  we see that the CM representation has the shortest range, which is one reason why it is easier to use than the other two representations.

In a similar fashion, the higher order interactions can be calculated from higher order probability distributions[5,11]. We calculated the relative strength of the many-body terms up to fifth order by computer simulations, and to arbitrary order by a scaling theory[11]. The simulations and the scaling theory agree well, and suggest that at full overlap the  $n$ th order many-body term alternates in sign as  $(-1)^n$ , and decreases (slowly) in absolute magnitude with increasing  $n$ . But, as mentioned before, a description based on three and higher order interactions rapidly becomes too unwieldy to use. Instead, we show in the next section how to derive a pair potential approach which includes these higher order ( $n > 2$ ) interactions in an average way.

## 2.2 Density-dependent polymer-polymer interactions

An alternative coarse-graining approach to the many-body expansion of the previous section is to find pair potentials which reproduce known structural information. We are aided in this by a theorem which states that at a given density  $\rho$ , there is a one-to-one mapping between the pair distribution function  $g(r)$  and a unique pair potential  $v(r; \rho)$  that will exactly reproduce the correct pair correlations[17]. We generate the pair correlations with simulations of SAW polymers, and at each density  $\rho$ , use the Ornstein-Zernike equations[15], coupled with the hypernetted-chain closure (HNC)[15], to invert the CM  $g(r)$  and find  $v(r; \rho)$ . While the HNC closure is generally not accurate enough for inversions in simple liquids, it is nearly exact for the soft potentials we are investigating here[5,6,18]. Nevertheless, there are a number of subtleties, both in the simulations and in the inversions, which must be carefully examined[10,12].

Density-dependent effective potentials  $v(r; \rho)$ , inverted from the  $g(r)$  produced by  $L = 500$  SAW simulations are shown in Fig. (3). The potential changes with increasing density, but approximately retains the shape found at  $\rho = 0$ . We have recently shown that these potentials can be very accurately parameterized for  $\rho/\rho^* < 2$  by sums of three Gaussians with density-dependent coefficients[12].

Within the HNC approximation, the density dependence of an effective pair potential that reproduces the true  $g(r)$  is given to lowest order in  $\rho$  and the  $w^{(n)}(\{\mathbf{r}_i\})$  by[19]:

$$v(r_{12}; \rho) = w^{(2)}(r_{12}) - \rho \int \left( e^{-\beta w^{(3)}(r_{12}, r_{13}, r_{23})} - 1 \right) g_2(r_{13}; \rho) g_2(r_{23}; \rho) d\mathbf{r}_3, (4)$$

We found that this expression describes the density dependence quite well for  $\rho/\rho^* < 1$ , and even works qualitatively for higher densities, where we expect higher order  $\rho$  and  $w^{(n)}(\{\mathbf{r}_i\})$  effects to become significant[11]. This demonstrates the connection between the density-independent and density-dependent approaches, showing explicitly that the density dependence in the effective pair-potentials  $v(r; \rho)$  arises from the many-body interactions.

One advantage of the structure-based route to the potentials is that one can use the compressibility equation[15] to derive the equation of state (EOS) from the pair correlations. We have done this for both  $L = 500$  and  $L = 2000$  SAW simulations. We directly measured the EOS and compared this to the EOS derived from the effective potentials through the compressibility equation[10,12]. The two routes are compared in Fig. 4, where the agreement is shown to be excellent.

All three effective potentials shown in Fig 2 result in “mean-field fluids” [5,6,18],

so named because the EOS takes on the mean-field form  $\beta\Pi/\rho \sim 1 + \rho\hat{v}(k=0)$  at high enough densities. Here  $\hat{v}(k)$  is the Fourier transform (FT) of the potential. This implies that if we only use the  $\rho = 0$  potential, then the EOS at higher density would scale as  $\beta\Pi/\rho \sim \rho$  instead of the correct  $\rho \sim \rho^{1.3}$  scaling found for the semi-dilute regime[13]. It is therefore the many-body interactions, expressed through the density dependence of  $v(r; \rho)$ , which cause the EOS to be super-linear.

We add a caveat here about the route to thermodynamics with density dependent potentials. The potentials derived here can be used to derive the correct thermodynamics through the compressibility route. Different (but related) density-dependent potentials, which do not reproduce the correct structure, would be needed to derive the correct thermodynamics through the virial route[19]. In other words, there is no unique density-dependent pair potential: when specifying such a potential, one must also specify which route to thermodynamics should be used[20].

### 3 Polymers near walls and spheres

Polymers form a depletion layer near a hard non-adsorbing wall because the number of possible conformations are restricted there. This is illustrated in Fig 6 for the CM and for a monomer representation near a planar wall. We have used an inversion method similar to that used in the previous sections to derive effective wall-polymer potentials for interacting polymers near walls and spheres[9,10,12]. These potentials are constrained to give the correct density profile  $\rho(r)$  which in turn determines the adsorption  $\Gamma$ . One can show, for example, that the surface tension is completely determined if one knows the EOS and  $\Gamma$  as a function of  $\rho$ [21]. Our effective polymer-polymer pair potentials correctly determine the EOS, while the wall-polymer potentials correctly determine  $\Gamma$ , implying that our formulation will reproduce the correct surface thermodynamics.

We show this adsorption  $\Gamma/\rho$  in Fig. 7, together with a simple fit constrained to give the correct scaling  $\Gamma/\rho \approx \xi(\rho) \sim \rho^{-0.77}$  in the semi-dilute regime. Note that the largest relative change in the adsorption is actually in the dilute regime, suggesting that even there descriptions based on the low-density or non-interacting polymer limit rapidly become inadequate.

## 4 Connection with scaling theory

Most successful theories of polymers start from a monomer based description and use scaling or RG approaches to derive properties of polymer solutions[13]. How does our CM based description compare with these scaling approaches? For example, in the semi-dilute regime, scaling theories predict that the important length-scale is the correlation length  $\xi(\rho)$ , which decreases with increasing density as  $\xi(\rho) \sim \rho^{-0.77}$ . It is not a-priori clear how this lengthscale enters into the  $g(r)$  or the  $v(r)$  in our description of homogeneous polymer solutions. The EOS scales as  $\beta\Pi/\rho \sim \xi^{-3}/\rho$  in the semi-dilute regime, a behaviour which is reproduced by our description through the compressibility equation. Since these potentials result in “mean-field fluids”, this suggests that  $\int dr r^2 v(r; \rho) \sim \xi^{-3}/\rho^2$  in the semi-dilute regime. For inhomogeneous systems in the semi-dilute regime,  $\xi$  enters more directly through the density profiles shown in Fig 6, but again the direct connection to the potentials is more opaque. So the exact connection with the scaling theory still remains to be worked out. We expect our approach to be most robust in the dilute regime and into the crossover region of the semi-dilute regime. Luckily this is also where much of the interesting physics of the colloid-polymer systems lies. How well our “soft colloids” approach will work deep into the semi-dilute regime still remains to be established.

## 5 Extensions to poor solvents and mixtures

The considerations in the previous sections focused on equal length polymers in a good solvent, where the temperature plays no role. However, the techniques used for polymers in a good solvent should still apply to other types of polymers solutions.

### 5.1 Poor solvents

We first examine briefly what happens for polymers in a poor solvent, using as a model SAW polymers with a nearest neighbor attraction of strength  $-\beta\epsilon$ . It is known that as the temperature decreases, there is a temperature  $T_{col}$  below which the polymer collapses into a compact globule and loses its fractal nature[13]. The effective potentials will then be fundamentally different of course. But as long as we stay above this temperature, we expect that the interaction should become less strong with decreasing temperature, as shown in Fig. 5.

## 5.2 Mixtures

Renormalization group (RG) calculations for the interaction between the CM of two polymers of differing lengths  $R_{g1}$  and  $R_{g2}$  suggest that the interaction strength at full overlap should weaken with increasing size asymmetry, and that the interaction range should approximately scale as  $R_{12} = \frac{1}{2}\sqrt{R_{g1}^2 + R_{g2}^2}$ [22]. We confirm this behaviour for simulations of a number of different length SAW polymers at  $\rho = 0$  in Fig. 5.

## 5.3 Phase separation?

An interesting prediction is that binary mixtures of Gaussian core particles interacting via the pair potentials  $V_{\alpha\beta}(r) = \epsilon_{\alpha\beta} \exp\{-(r/R_{\alpha\beta})^2\}$  will phase-separate over broad ranges of the coupling constant ratio  $|\epsilon_{12}|/\sqrt{\epsilon_{11}\epsilon_{22}}$ . Semi-quantitative correct phase-diagrams follow already from an analytic mean-field calculation[23], and suggest that polymers in a good solvent will not phase separate at low densities.

## 5.4 Relationship with PRISM

Each time the present coarse-graining methods are applied to a new type of polymer solution we need a new set of computer simulations at the monomer level for the parameters of interest. It would be very helpful to find other, semi-analytic, ways of providing input information that are faster and more flexible. One candidate would be PRISM[24], an integral equation method which has been applied to a wide variety of polymeric systems. This requires a way of deriving CM-CM correlations from the monomer based correlations provided by PRISM. As a first step in this direction, we have derived an approximate relationship which is much more accurate than earlier, heuristic approaches[25]. This could form the basis for using PRISM or other monomer based methods as input to our “polymers as soft colloids” approach.

## 6 Conclusions

In summary then, we have shown how to coarse-grain polymers as single “soft colloids”, with just three degrees of freedom each, interacting via a density-independent pair, triplet, and higher body potentials. These, however, become rapidly intractable. In parallel, we also derived density-dependent pair poten-



tials which include, in an average way, the effect of the higher  $n$ -body interactions. These effective pair potentials exactly reproduce the two-body correlations of the underlying polymer solution, and, through the compressibility equation, they reproduce the EOS as well. In a similar way the effective one-body potentials which exactly reproduce the one-body density profiles near walls and spheres can also be derived. Because these reproduce the correct adsorptions, the thermodynamics of a polymer solution near a non-adsorbing surfaces are also correctly reproduced by our formulation.

We also showed how to extend these methods to derive effective potentials for polymers in a poor solvent and for mixtures of different length polymers. We sketched some ways in which other monomer based methods such as PRISM could be used as the source of input to derive our potentials.

At this point one might ask what has been gained, since at each point direct computer simulations were needed as input to derive the potentials. This question brings us back to the aim stated at the outset: to describe mixtures of many polymers and many colloids. Here our coarse-graining of polymers as soft colloids does result in important simplifications. For example, we have performed such simulations for mixtures of spheres of radius  $R_c$  and polymers with sizes ranging from  $R_g/R_c \approx 0.3$  to  $R_g/R_c \approx 1$ , and determined the polymer induced phase-separation of the colloids[26]. The effective polymer density  $\rho/\rho^*$  at the critical point increases with increasing polymer size, but even for the largest polymers it is still in the regime  $\rho/\rho^* \leq 1$ , where we expect our formulation to work best. Simulations with a full polymer model would be about two orders of magnitude slower. Without coarse-graining the polymers as soft colloids, such a simulation would have been virtually impossible to perform.

## Acknowledgements

AAL acknowledges support from the Isaac Newton Trust, Cambridge, PB and VK acknowledge support from the EPSRC under grant number GR/M88839, RF acknowledges support from the Oppenheim Trust, EJM acknowledges support from the Royal Netherlands Academy of Arts and Sciences. EJM acknowledges support from the Stichting Nationale Computerfaciliteiten (NCF) and the Nederlandse Organisatie voor Wetenschappelijk Onderzoek (NWO) for the use of supercomputer facilities.

## References

- [1] W.B. Russel, D.A. Saville, and W.R. Schowalter, *Colloidal Dispersions*, Cambridge University Press, Cambridge (1989).
- [2] H.N.W. Lekkerkerker, W.C.K. Poon, P.N. Pusey, A. Stroobants and P.B. Warren, Europhys. Lett. **20**, 559 (1992).
- [3] E.J. Meijer and D. Frenkel, J. Chem. Phys. **100**, 6873 (1994).
- [4] See e.g. W. C. K. Poon, *et al.*, Phil. Trans. Roy. Soc. A **359**, 897 (2001); H. Löwen, *et al.*, *ibid*, 909; A. Yodh *et al.*, *ibid*, 921; R. Evans, *et al.*, *ibid*, 961 (2001), for some short reviews.
- [5] A.A. Louis, Phil. Trans. Roy. Soc. A **359**, 939 (2001).
- [6] C.N. Likos, Phys. Rep. **348**, 267 (2001).
- [7] S. Asakura and F. Oosawa, J. Polym. Sci., Polym. Symp. **33**, 183 (1958), A. Vrij, Pure Appl. Chem. **48**, 471 (1976).
- [8] A. A. Louis, R. Finken, and J.P. Hansen Europhys. Lett., **46**, 741 (1999).
- [9] A.A. Louis, P.G. Bolhuis, J.P. Hansen and E.J. Meijer, Phys. Rev. Lett. **85**, 2522 (2000).
- [10] P.G. Bolhuis, A.A. Louis, J-P Hansen and E.J. Meijer, J. Chem. Phys. **114**, 4296 (2001).
- [11] P.G. Bolhuis, A.A. Louis, and J-P Hansen, Phys. Rev. E **64**, 021801 (2001).
- [12] P.G. Bolhuis and A.A. Louis, to appear in Macromolecules.
- [13] P.G. de Gennes, *Scaling Concepts in Polymer Physics* (Cornell University Press, Ithaca NY, 1979).
- [14] A.Y. Grosberg, P.G. Khalatur, and A.R. Khokhlov, Makromol. Chem., Rapid Commun. **3**, 709 (1982).
- [15] J.P. Hansen and I.R. McDonald, *Theory of Simple Liquids, 2nd Ed.* (Academic Press, London, 1986).
- [16] In our earlier work[9–11] we used  $R_g = 16.5$  instead of the correct  $R_g = 16.83$  value for the  $L = 500$  SAW polymers. This means a slight adjustment in the values of  $R_g$  and in  $\rho/\rho^*$  quoted in our papers. For example, the values quoted for  $\rho/\rho^*$  should increase by a factor 1.06.
- [17] R.L. Henderson, Phys. Lett. A. **49**, 197 (1974); J.T. Chayes and L. Chayes, J. Stat. Phys., **36**, 471 (1984); L. Reatto, Phil. Mag. A **58**, 37 (1986).
- [18] A.A. Louis, P. Bolhuis, and J.P. Hansen, Phys. Rev. E. **62**, 7961 (2000); C.N. Likos, A. Lang, M. Watzlawek, and H. Löwen, *ibid* **63**, 031206 (2001).
- [19] see e.g. M.A. van der Hoef and P.A. Madden, J. Chem. Phys. **111**, 1520 (1999), and references therein.
- [20] A.A. Louis, manuscript in preparation (2001)

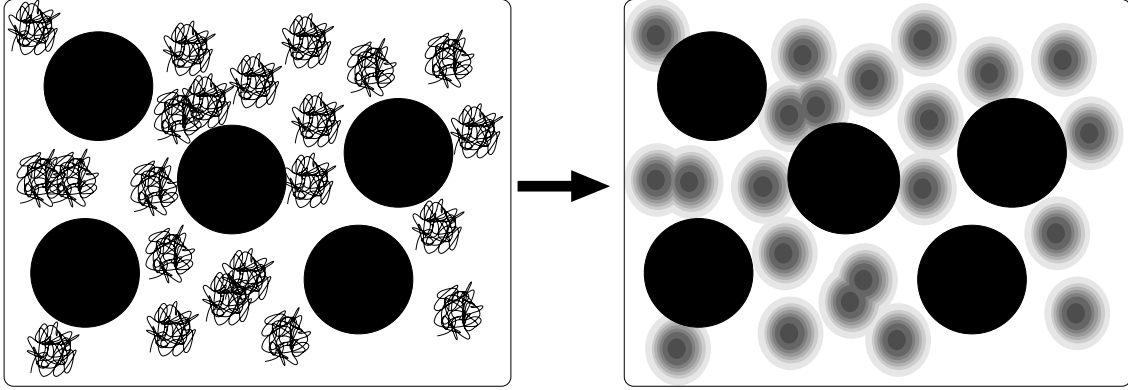


Fig. 1. Schematic picture of our coarse-graining scheme: The polymers in a polymer-colloid mixture are treated as single entities, on the same footing as the colloidal particles.

- [21] Y. Mao, P. Bladon, H.N.W. Lekkerkerker and M.E. Cates, *Mol. Phys.* **92**, 151 (1997)
- [22] B.Krüger, L. Schäfer, and A. Baumgärtner, *J. Phys. France* **50**, 319 (1989).
- [23] R. Finken, J.P. Hansen, and A.A. Louis, cond-mat/011034, to appear in *J. Stat. Phys.*; A.J. Archer and R. Evans, *Phys. Rev. E* **64**, 041501 (2001)
- [24] K.S. Schweitzer and J. Curro, *Adv. Chem. Phys.* **98**, 1 (1997).
- [25] V. Krakoviack, J.P. Hansen, and A.A. Louis, cond-mat/0110387.
- [26] P.G. Bolhuis, A.A. Louis, and J.P. Hansen, manuscript in preparation.

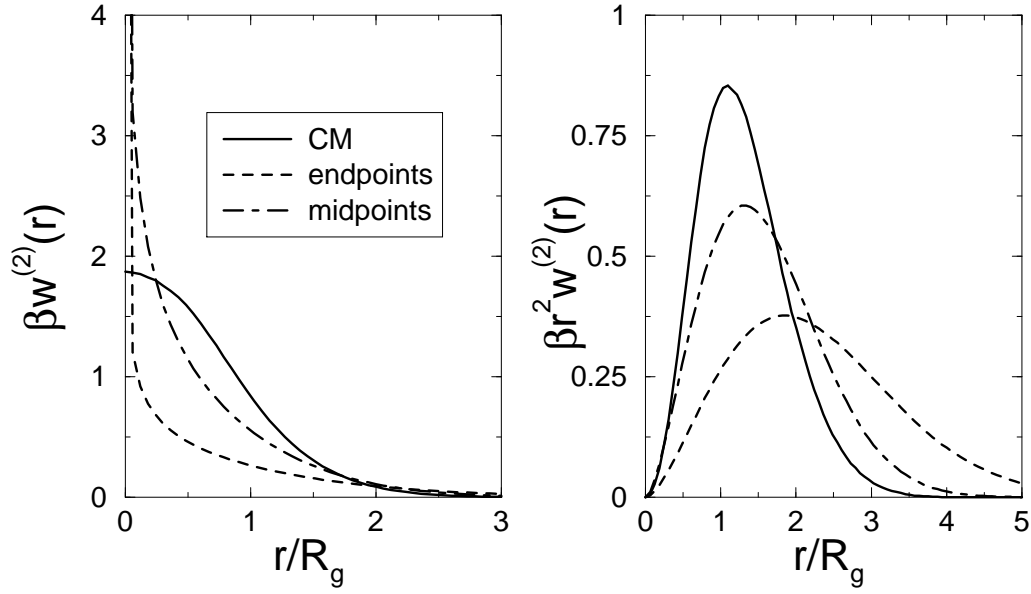


Fig. 2.  $w^{(2)}(r)$  and  $r^2 w^{(2)}(r)$  for the interaction between two isolated polymers in the CM, end-point, and mid-point representations. The end-point and mid-point potentials diverge at the origin, but the CM representation gives a finite value. All three potentials result in the same second virial coefficient  $B_2$  defined in Eq. (1).

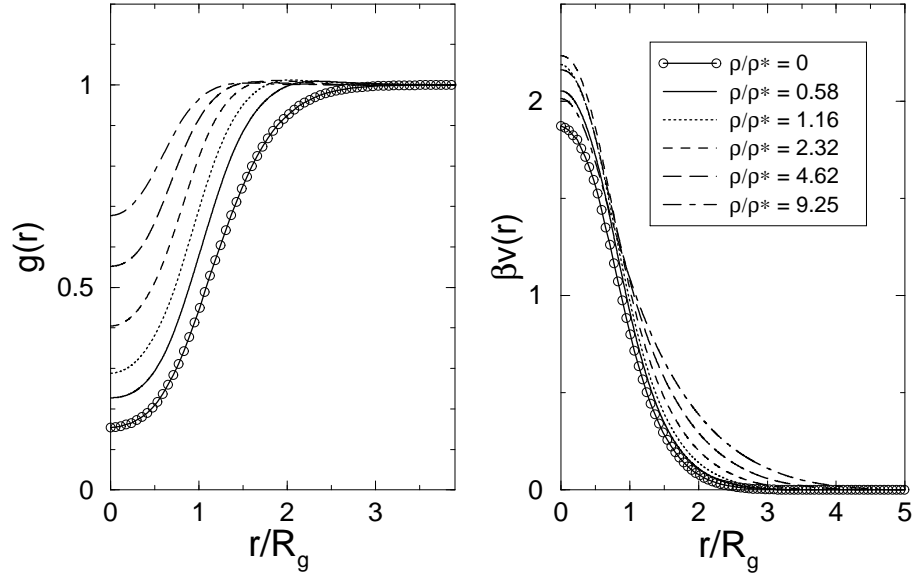


Fig. 3. The effective polymer pair potentials  $v(r; \rho)$ , derived at different densities from an HNC inversion of the CM pair distribution functions  $g(r)$  of  $L = 500$  SAW polymer coils. (from Ref[11])

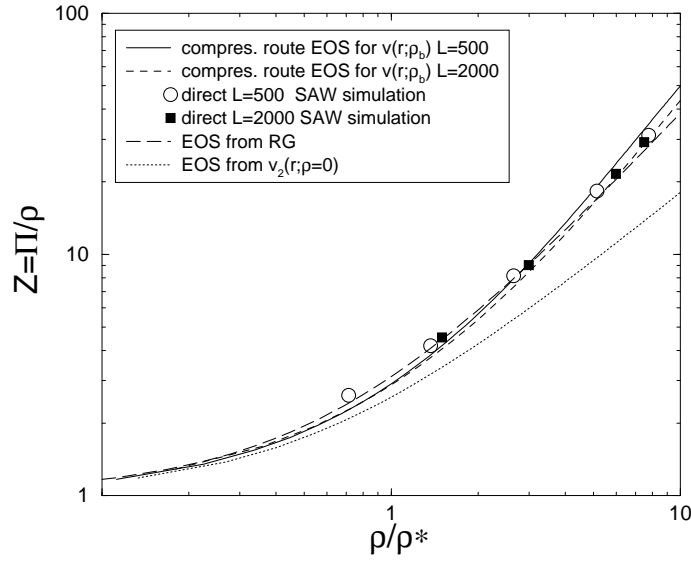


Fig. 4. EOS for polymers in good solvent. Direct results and the EOS arising from the effective potentials through the compressibility route are compared for  $L = 500$  and  $L = 2000$  SAW polymers.

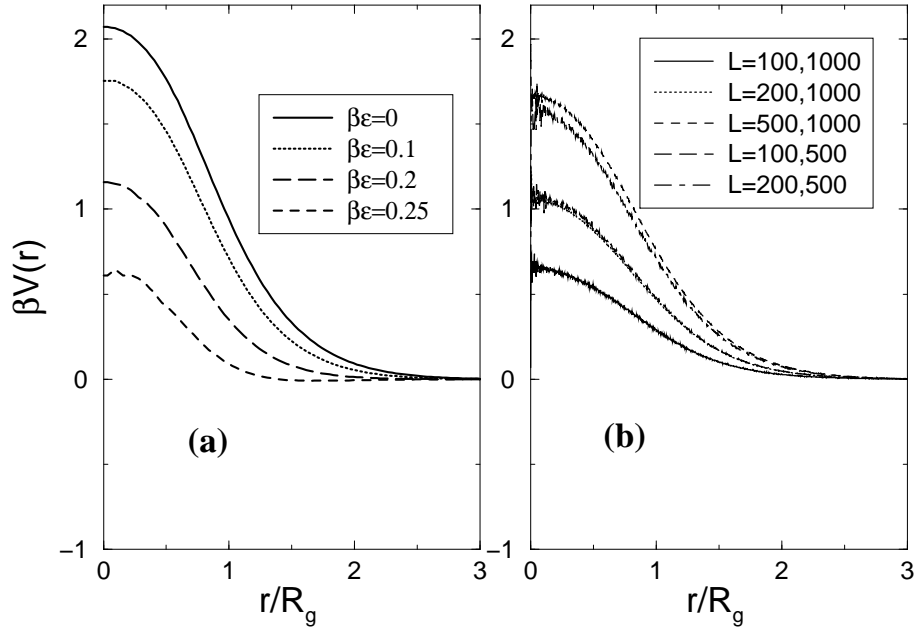


Fig. 5. **(a)** CM-CM interaction for polymers in a poor solvent, modeled by  $L = 100$  SAW polymers on a cubic lattice with nearest neighbour attractions of strength  $-\beta\epsilon$ . **(b)** CM-CM interaction for mixtures of different length SAW polymers.

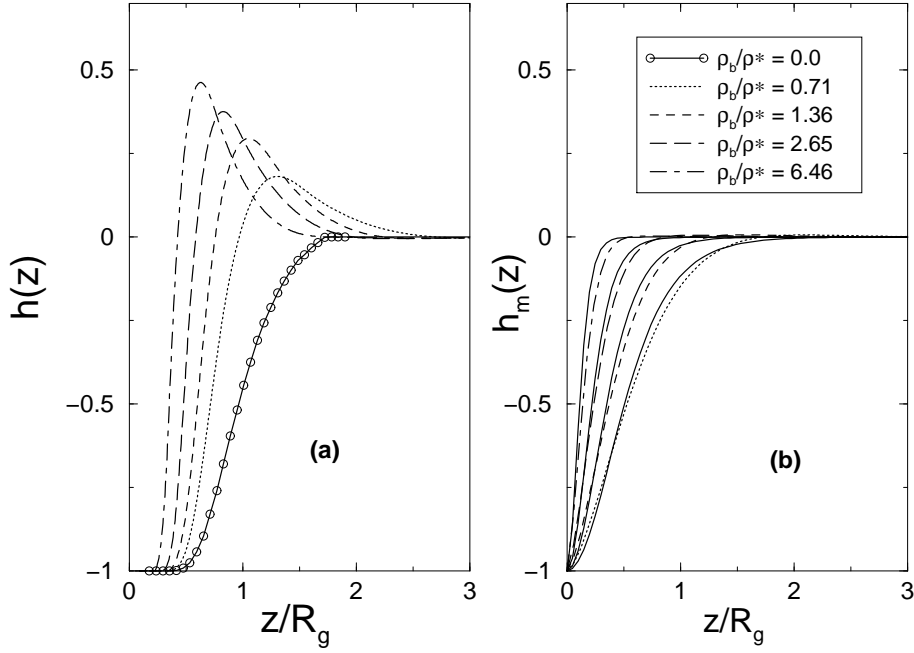


Fig. 6. **(a)** The wall-polymer CM profile  $h(z) = \rho(z)/\rho - 1$  for  $L = 500$  SAW polymers at different bulk concentrations. **(b)** The wall-polymer monomer profile  $h_m(z)$  for the same bulk concentrations. Both representations result, by definition, in the same relative adsorptions  $\Gamma/\rho$ . The straight lines in **(b)** are a fit to the simple form  $h_m(z) = \tanh^2(-z\rho/\Gamma(\rho)) - 1$ [13]

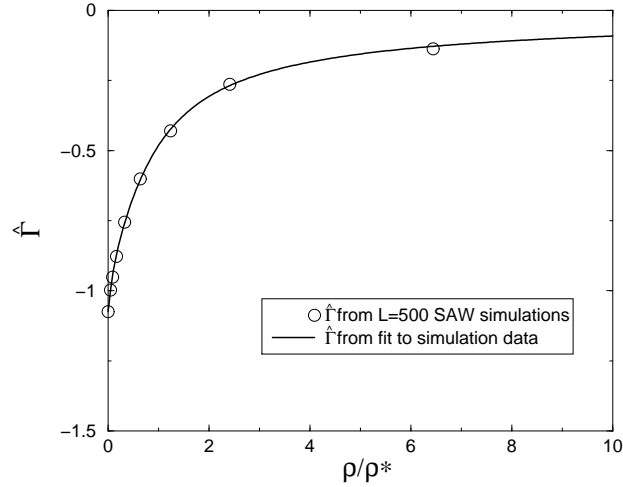


Fig. 7. Relative adsorption  $\Gamma/\rho$ , in units of  $R_g$  of  $L = 500$  SAW polymers near a single hard wall. Circles are direct simulations and the line denotes the simple fit with the correct scaling behavior, given by  $\hat{\Gamma}(\rho) = -1.074R_g \left(1 + 7.63\frac{\rho}{\rho^*} + 14.56\left(\frac{\rho}{\rho^*}\right)^3\right)^{-(0.2565)}$